

# **The use of non-functional clonotypes as a natural calibrator for quantitative bias correction in adaptive immune receptor repertoire profiling**

Anastasia Smirnova<sup>1,2</sup>, Anna Miroshnichenkova<sup>1,3</sup>, Yulia Olshanskaya<sup>1,3</sup>, Michael Maschan<sup>2</sup>, Yuri Lebedev<sup>1,4</sup>, Dmitriy Chudakov<sup>1,4,5,6</sup>, Ilgar Mamedov<sup>1,4</sup>, Alexander Komkov<sup>1,3,6\*</sup>

<sup>1</sup> Department of Genomics of Adaptive Immunity, Shemyakin-Ovchinnikov Institute of Bioorganic Chemistry, Moscow, Russia.

<sup>2</sup> Skolkovo Institute of Science and Technology, Moscow, Russia

<sup>3</sup> Dmitry Rogachev National Medical and Research Center of Pediatric Hematology, Oncology and Immunology, Moscow, Russia.

<sup>4</sup> Department of Molecular Technologies, Pirogov Russian National Research Medical University, Moscow, Russia

<sup>5</sup> Central European Institute of Technology, Masaryk University, Brno, Czech Republic

<sup>6</sup> MiLaboratory LLC, Moscow, Russia

\*Correspondence: [alexandrkomkov@yandex.ru](mailto:alexandrkomkov@yandex.ru)

## **Abstract**

High-throughput sequencing of adaptive immune receptor repertoires is a valuable tool for receiving insights in adaptive immunity studies. Several powerful TCR/BCR repertoire reconstruction and analysis methods have been developed in the past decade. However, detecting and correcting the discrepancy between real and experimentally observed lymphocyte clone frequencies is still challenging. Here we discovered a hallmark anomaly in the ratio between read count and clone count-based frequencies of non-functional clonotypes in multiplex PCR-based immune repertoires. Calculating this anomaly, we formulated a quantitative measure of V- and J-genes frequency bias driven by multiplex PCR during library preparation called Over Amplification Rate (OAR). Based on the OAR concept, we developed an original software for multiplex PCR-specific bias evaluation and correction named iROAR: Immune Repertoire Over Amplification Removal (<https://github.com/smiranast/iROAR>). The iROAR algorithm was successfully tested on previously published TCR repertoires obtained using both 5' RACE (Rapid Amplification of cDNA Ends)-based and multiplex PCR-based approaches and compared with a biological spike-in-based method for PCR bias evaluation. The developed approach can increase the accuracy and consistency of repertoires reconstructed by different methods making them more applicable for comparative analysis.

## **Introduction**

Adaptive immune receptor (TCR – T-cell receptor and BCR – B-cell receptor) repertoire is usually defined as a set of TCR or BCR sequences obtained from an individual's blood, bone marrow, or specific lymphocyte population. Reflecting the T/B cell's clonal composition, the

41 repertoire is characterized by a high degree of specificity for each individual and substantial  
42 variation in clone frequencies. The accuracy of both sequences and frequencies of TCR/BCR  
43 genes in the obtained repertoire is essential to receiving the correct biological information from  
44 immune repertoire analysis.

45 High-throughput sequencing (HTS) of adaptive immune receptor repertoires is widely  
46 used in immunological studies (reviewed in (Minervina et al., 2019)) for the investigation of  
47 immune response to vaccines (Minervina et al., 2021; Pogorelyy et al., 2018; Sycheva et al.,  
48 2022), tumor-infiltrating lymphocytes (Gee et al., 2018; Goncharov et al., 2022; Oliveira et al.,  
49 2021), new therapeutic agents (Huang et al., 2019; Wang et al., 2018; Wilson et al., 2022),  
50 leukemia clonality and minimal residual disease monitoring (Brüggemann et al., 2019; Komkov  
51 et al., 2020; Nazarov et al., 2016; Tirtakusuma et al., 2022; Wood et al., 2018). HTS-based  
52 methods for immune repertoire profiling use either RNA or DNA as a starting material and, in  
53 most cases, use PCR for the selective enrichment of receptor sequences. DNA-based methods  
54 generally use two-sided multiplex PCR with primers annealing to multiple V- and J-genes of the  
55 rearranged receptor (Brüggemann et al., 2019; Komkov et al., 2020; Robins et al., 2009). RNA-  
56 based methods start with cDNA synthesis, usually with TCR/BCR C(constant)-genes specific  
57 oligonucleotides, followed by one-side multiplex amplification with a set of V-gene specific  
58 primers and a universal C-gene specific primer (Wang et al., 2010). Alternatively, two universal  
59 primers are used for amplification if an artificial sequence is added to the 5' end during synthesis  
60 using a template-switch (5'-RACE) (Mamedov et al., 2013) or ligation (Oakes et al., 2017).  
61 DNA-based methods protect the repertoire from gene transcription bias and provide more  
62 comprehensive results (Barennes et al., 2020) which include most non-functional (out-of-frame)  
63 as well as functional (in-frame) rearrangements but produce high amplification bias in the course  
64 of multiplex PCR. Additionally, each T/B cell contains a single DNA copy (i.e., two target  
65 strands) of the receptor molecule in contrast to tens of single-stranded RNA copies. RNA-based  
66 methods using 5'-RACE or ligation are characterized by the lowest PCR bias as they need a  
67 single primer pair for the amplification. However, the low efficiency of adding a universal oligo  
68 to the 5'-end makes its sensitivity comparable to or even lower than DNA-based methods. The  
69 compromise between these two approaches is the RNA-based method with a one-side multiplex  
70 that has moderate amplification bias yet sufficient sensitivity (Ma et al., 2018). Most bias in one-  
71 side multiplex RNA-based approaches could be removed by using unique molecular identifiers  
72 (UMI) (Ma et al., 2018). Unfortunately, for DNA-based methods, efficient incorporation of  
73 UMIs into the initial molecule before PCR is still challenging. The only method for DNA  
74 multiplex bias correction (Carlson et al., 2013) is undirected and cost-ineffective due to the  
75 utilization of an expensive synthetic spike-in control repertoire. Here we propose an orthogonal  
76 solution for this challenge: the first fully computational algorithm for amplification bias  
77 detection and correction in adaptive immune receptor repertoires named iROAR (immune  
78 Repertoire Over Amplification Removal).

79

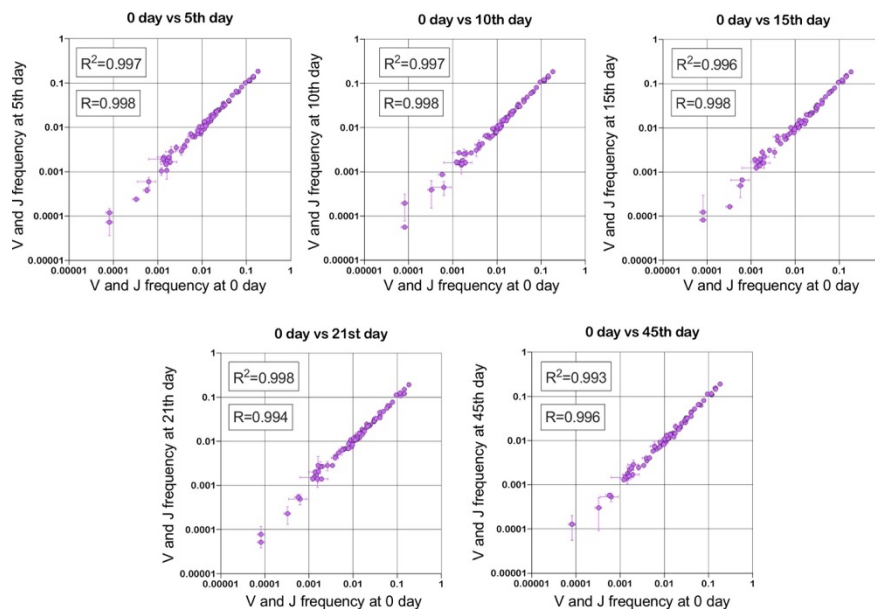
80

## Results

## 81 The rationale for the Over Amplification Rate measure

82 Since out-of-frame TCR/BCR rearrangements do not form a functional receptor, they are  
83 not subjected to any specific clonal expansions and selection (Murugan et al., 2012). Being a  
84 passenger genomic variation, they change their initial (recombinational) clonal frequencies just  
85 randomly following the frequency changes of the second functional (in-frame) TCR/BCR allele  
86 present in the same T/B cell clone. According to the TCR/BCR loci rearrangement mechanism,  
87 the formation of in-frame and out-of-frame allele combinations in the same cell is also a  
88 stochastic and independent process in terms of V- and J-genes frequency. It leads to the  
89 conclusion that V- and J-gene frequencies among out-of-frame rearrangements must be  
90 sufficiently stable and must be equal to the initial recombination frequencies despite repertoire  
91 changes caused by various immune challenges (Fig 1). Thus, reproducible deviation of out-of-  
92 frame V- and J-gene frequencies (for the same multiplex PCR primer set) from the initial  
93 recombinational frequencies observed in the sequenced repertoire dataset is a result of artificial  
94 aberration caused by PCR amplification rather than immune repertoire evolution. Thus out-of-  
95 frame clonotypes can be considered a natural calibrator that can be used to measure amplification  
96 bias and quantitatively correct immune repertoire data.

97



98

99

100 **Figure 1.** Stability of TRBV and TRBJ genes frequencies calculated based on unique out-of-  
101 frame rearrangements after Yellow fever vaccination (model of acute viral infection). Out-of-  
102 frame clonotypes for frequencies calculation were extracted from low-biased 5' RACE TRB  
103 repertoires of PBMC samples obtained in two replicates for six time points: 0, 5, 10, 15, 21, and  
104 45 days after YFV injection (donor M1, SRA accession number PRJNA577794 (Minervina et al.,  
105 2020)).

106

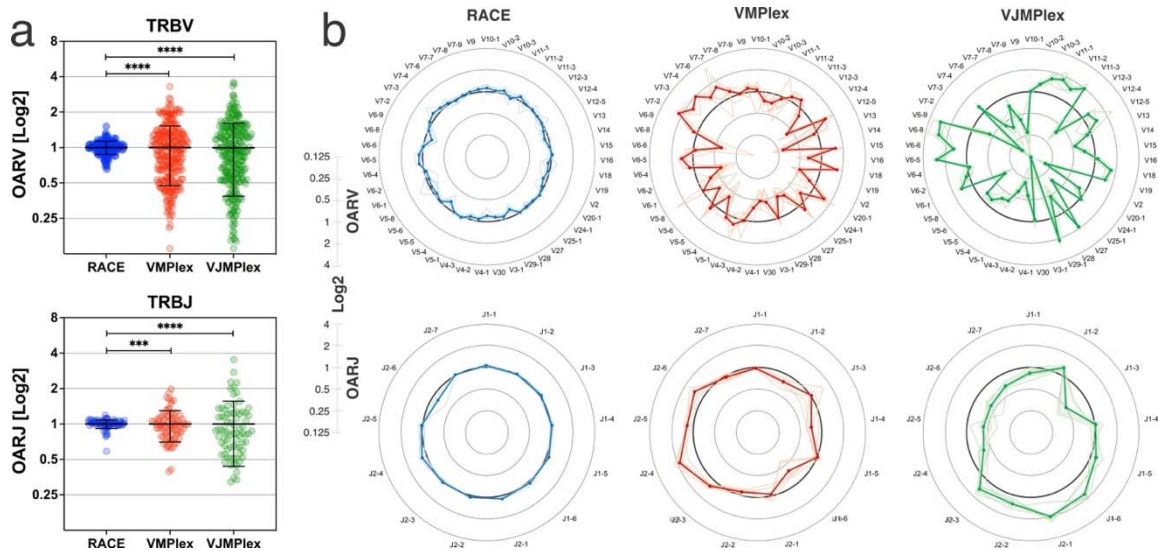
107 Formulating this observation, we developed the Over Amplification Rate (OAR)  
 108 measure, which we define as a ratio of the observed and expected frequency of a V- (OAR(Vi))  
 109 or a J-gene (OAR(Ji)) among identified out-of-frame rearrangements. Observed frequency  
 110 represents a value calculated as read counts (RC) for each V- and J-gene (related to out-of-  
 111 frames) divided by the sum of all out-of-frame clones read count in the obtained repertoire  
 112 sequencing dataset. The expected frequency is a value before amplification calculated as a  
 113 number of unique out-of-frame clones (UCN) having each V- or J-gene divided by the total  
 114 number of unique out-of-frame clones in the repertoire. At the final stage each OAR is  
 115 normalized by dividing by the average OAR.

$$OAR(Vi) = \frac{RC(Vi) / \sum_1^N RC(Vi)}{UCN(Vi) / \sum_1^N UCN(Vi)}$$

$$OAR(Ji) = \frac{RC(Ji) / \sum_1^N RC(Ji)}{UCN(Ji) / \sum_1^N UCN(Ji)}$$

116  
 117  
 118  
 119  
 120  
 121

OAR value tends to be equal to 1 under ideal conditions (low or no amplification bias). It deviates from 1 as amplification bias increases in line: 5'-RACE with a single universal primer pair, one-side multiplex PCR (VMplex), and two-side multiplex PCR (VJMplex) (Fig 2).



122  
 123 **Figure 2.** a. Comparison of OAR values variances for TRB repertoires obtained with 5'-RACE,  
 124 one-side multiplex (VMplex), and two-side multiplex (VJMplex) PCR. The Levene's test was  
 125 performed to compare OAR variances: \*\*\*\* $P < 0.0001$ , \*\*\* $P < 0.001$ . The bar and whiskers

126 indicate a mean and standard deviation. *b*. Average (bold lines) OAR values for TRBV and TRBJ  
127 genes in repertoires obtained with 5'-RACE, one-side multiplex (VMplex), and two-side  
128 multiplex (VJMplex) PCR. Pale lines illustrate OARs of individual repertoires. Datasets: six  
129 repertoires for RACE from PRJNA847436 (Sycheva et al., 2022), six repertoires for  
130 VMplex from PRJNA427746 (Ma et al., 2018), six repertoires for VJMplex from  
131 27483#.XpCuQ1MzZQI (zenodo.org) (Weinberger et al., 2015).

132

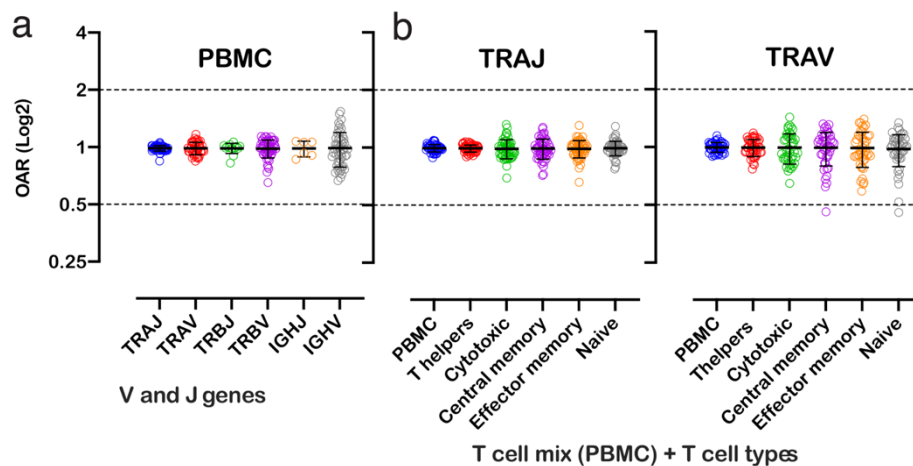
### 133 The versatility of OAR measure

134 OAR measurement is a universal approach and can be applied to different types of immune  
135 repertoire data. To demonstrate this versatility, we calculated OAR values for low-biased (5'  
136 RACE) repertoires of different adaptive immune receptor chains obtained from bulk human  
137 PBMC: TCR alpha (TRA), TCR beta (TRB), and BCR heavy chains (Fig. 3a). The results show  
138 that OARs for both TCR and BCR repertoires obtained by 5' RACE are close to 1 and stay  
139 within the range of 0.5 to 2, which is much narrower than OAR for multiplex PCR-based  
140 repertoires (see main text Fig. 2).

141 We also analyzed OARs for low-biased (5' RACE) TCR repertoires of different T cell  
142 subpopulations, including T-helper, cytotoxic, central memory, effector memory, and naïve T  
143 cells. As shown in Fig. 3, the OAR values demonstrate much less differences between analyzed  
144 T cell types than between RACE and multiplex PCR and are close enough to 1 similarly to the  
145 repertoire of bulk T cell mix obtained from PBMC.

146 Herewith, the variance of IGHV's OARs compared TCRs' and the variance of TCR  
147 subpopulations OARs compared PBMCs' is slightly higher. This phenomenon may be linked to  
148 well-known differences in clonal expansion intensities of B/T-cell subsets which can affect  
149 indirectly the OAR values. However, the proof of this hypothesis demands separate deep  
150 analysis which is beyond the main focus of this research.

151 Despite it, our results demonstrate that OAR is a sufficiently universal measure of  
152 repertoires and can be applied to most adaptive immune receptors and cell types.



153

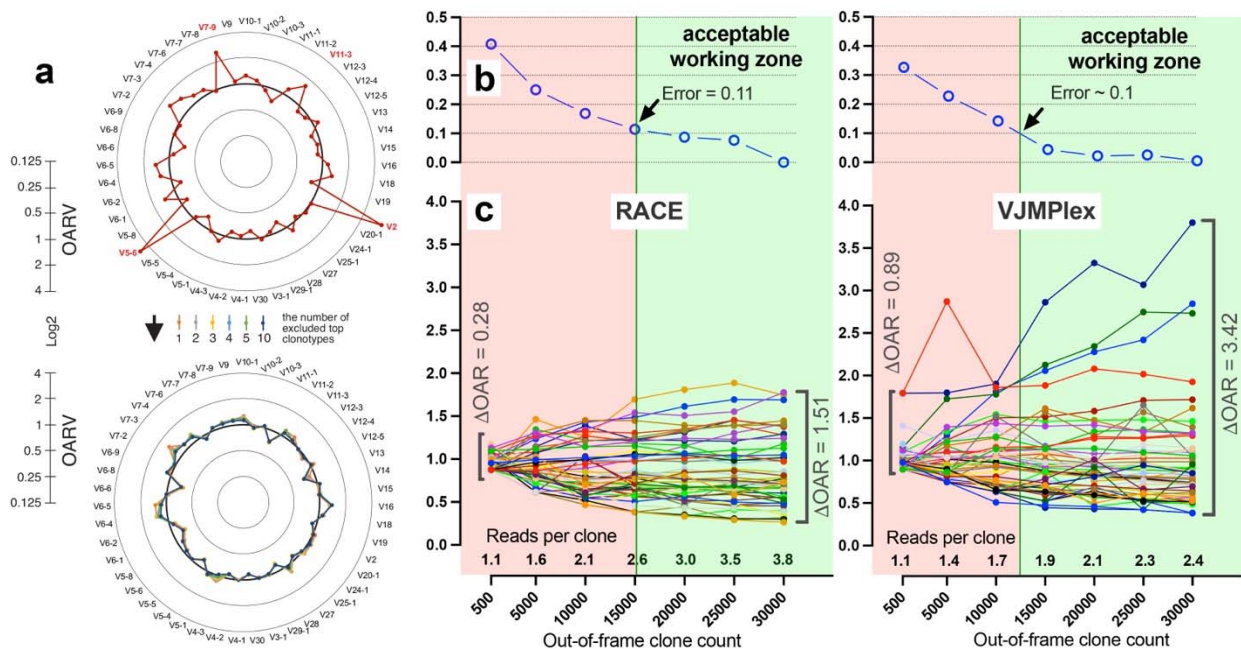
154 **Figure 3.** Distribution of Over Amplification Rates of V- and J-genes in RACE-based repertoires  
155 of TCR and BCR (the empty dots represent average OARs among TCR repertoires: SRA

156 *accession numbers: PRJNA577794, PRJNA316572, PRJEB27352, and BCR repertoires: SRA*  
 157 *accession number: PRJNA297771, PRJNA494572).* B. Over Amplification Rates of V- and J-  
 158 *genes of TCR alpha chains in RACE-based repertoires of different types of T-cells (donors M1*  
 159 *and P30, 45<sup>th</sup> day after booster vaccination, SRA accession number PRJNA577794 (Minervina et*  
 160 *al., 2020))* The bar and whiskers indicate a mean and standard deviation.

### 161 162 **Factors affecting OAR measure accuracy**

163 In the case of insufficient sequencing coverage, high PCR bias can lead to the dramatic  
 164 loss of clones and thus an incorrect measurement of V- and J-genes frequencies. In this instance,  
 165 for the majority of V- and J-genes, the population frequencies can approximate the real  
 166 frequencies better than multiplex repertoire-based ones (Suppl Fig 1). If upon comparison  
 167 samples' UCN-based frequencies significantly differ from the average frequencies calculated for  
 168 the population (i.e., exceeds 99% confidence interval), OAR calculation should be based on the  
 169 latter.

170 Also, the balance of V- and J-genes frequencies can be disrupted by accidentally arisen  
 171 abnormally large non-functional clonotypes generated in the course of abnormal clonal  
 172 expansion in various lymphoproliferative disorders or stochastic spike in normal lymphocyte  
 173 population. To reduce the impact of this anomaly on OAR value, the top clone of each V and J-  
 174 gene containing subgroups must be excluded from OAR calculation. Since V- and J-specific bias  
 175 affects all clones non-selectively, the remaining large part of clones after top clones exclusion  
 176 should be still representative for PCR bias calculation. As shown in Fig4a, the exclusion of one  
 177 top clonotype from OAR calculation for RACE-based TRB repertoire is enough to restore OAR  
 178 calculation accuracy for TRBV2, TRBV5-6, TRBV7-9, TRBV11-3. The further top clones  
 179 exclusion has no significant effect on OAR values.



180

181 **Figure 4.** Factors impacting OAR calculation accuracy. a. Impact of highly proliferated top non-  
182 functional clonotype on OAR calculation accuracy in low-biased RACE-based TRB repertoire  
183 (Data: SRR19594184). b. Impact of sequencing depth on OARs calculation error. c. PCR bias  
184 independent changes of TRB V-genes OARs as a function of sequencing depth. Data: two-sided  
185 multiplex-based TRB repertoire (Data: RACE - SRR3129976, VJMplex – SRR3129972).

186  
187 Another aspect impacting the accuracy of OAR calculation is the low sequencing  
188 coverage of the TCR/BCR repertoire. The ratio of total read counts and the sum of unique clone  
189 counts can affect OAR value despite PCR bias solely because of the mathematical properties of  
190 the OAR formula. In the extreme case, the OAR value ( $OAR = 1$ ) for V- and J-genes represented  
191 in a single out-of-frame clone with only one read will not reflect the real amplification bias. To  
192 address this issue, we analyzed the OAR calculation error as a function of the number of reads  
193 per clone used for the OARs evaluation (Fig. 4b). For this purpose, we performed a serial down-  
194 sampling of TCR datasets generated by RACE and two-side multiplex PCR and calculated OAR  
195 measurement error for each dataset portion. OAR calculated for the entire dataset was taken as a  
196 benchmark. The result shows that 1.8 (for Mplex) and 2.5 (for RACE) reads per out-of-frame  
197 clonotype are a minimal sufficient sequencing coverage to get adequate OAR values with an  
198 acceptable error rate of ~10%.

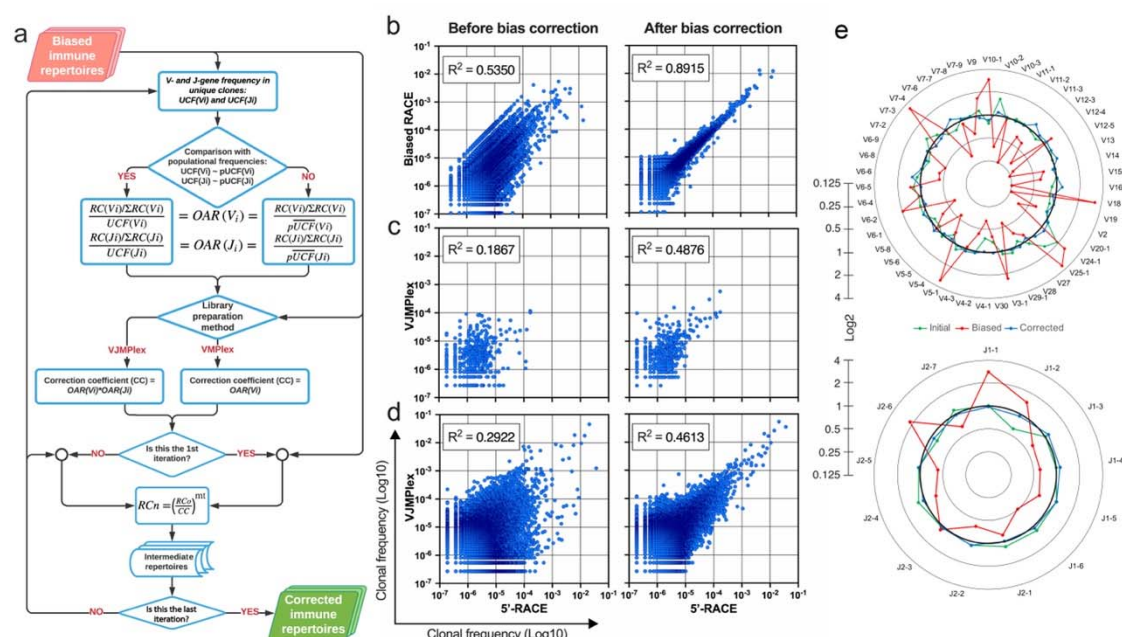
199 It is also important to note that errors in nucleotide sequences occurring during library  
200 preparation and sequencing could lead to an artificial increase in both in-frame and out-of-frame  
201 clone diversity. Single nucleotide substitutions generate artificial clones as a branch of real most  
202 abundant clones inside of each in-frame and out-of-frame group independently. Single nucleotide  
203 indels lead to cross-generation artificial clones between groups: real in-frame clones generate  
204 false out-of-frame clones and vice versa. Artificial clones compromise the accuracy of both  
205 repertoire itself and OAR value. To eliminate such clones generated by single-nucleotide  
206 substitutions, we filtered them out by the VDJTOOLS software (see Methods section). To  
207 eliminate artificial clones produced by indels, we searched for in-frame and out-of-frame clone  
208 pairs which differ by one indel (Levenshtein distance = 1). If their ratio is less than 1:500, the  
209 smaller clone in pair is discarded, and its count is added to the count of the larger clone (this  
210 procedure guarantees to discard most sequencing errors present in 1 per 1000 nucleotides  
211 average).

212  
213 **Over amplification rate index**

214 To estimate the value of immune repertoire structure disruption by amplification bias, we  
215 proposed the OAR-index, which represents the mean square deviation of OARs for each V and J  
216 gene from the value characteristic for repertoire with no bias ( $OAR=1$ ). OAR-index is directly  
217 proportional to the amplification bias and thus can be used for rapid estimation and comparison  
218 of immune repertoire bias. The less OAR index is, the less PCR bias is with an ideally unbiased  
219 repertoire having OAR-index = 0.

$$OAR - index = \sqrt{\frac{\sum_0^n (OAR_i - 1)^2}{n}}$$

220  
 221 **Using OAR for the removal of amplification bias**  
 222 Normalization coefficients for each V-J combination are estimated by multiplication of  
 223 corresponding V- and J-gene OARs for two-side multiplex and V-gene OAR for one-side  
 224 multiplex (Fig 2a). The corrected read count for each clonotype with the particular V-J gene  
 225 combination is obtained simply by dividing the observed read count by the corresponding  
 226 normalization coefficient. OAR of V- and J-genes could be co-dependent, which can be a reason  
 227 for overcorrection. To avoid this issue, the procedure can be recursively repeated with a modified  
 228 normalization coefficient defined as described coefficient raised to the power of a number in the  
 229 range from 0 to 1 (parameter “mt”). The corrected read counts are used to estimate the real  
 230 percentage of each clonotype in the repertoire. However, the all multiplex-based repertoires  
 231 analyzed in actual study required just 1 iteration with  $mt = 1$ . A detailed flowchart of the OAR-  
 232 based amplification bias correction algorithm named iROAR is shown in Fig 5a.



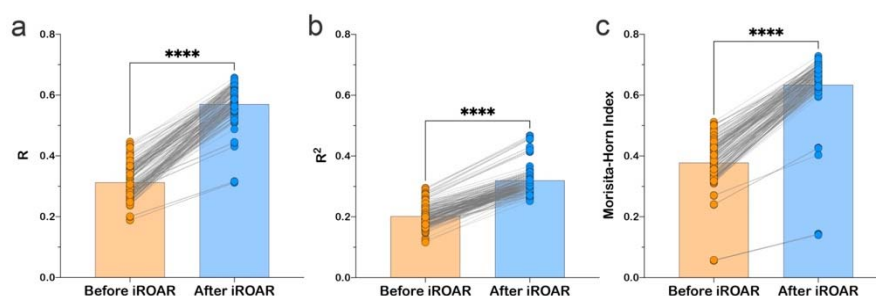
233  
 234 **Figure 5.** a. Flowchart of iROAR algorithm. UCF – Frequency calculated using unique clones  
 235 counts (denominator of OAR), pUCF – population UCF, RC – read count, RCn – normalized  
 236 RC, RCo – observed RC, mt – the number in the range from 0 to 1 for the iterative procedure. b.  
 237 Clone frequencies in the low biased 5'-RACE-based repertoire (ENA database, accession  
 238 number ERR2869430) versus the same repertoire with introduced artificial bias: before and  
 239 after iROAR processing. c. Out-of-frame (non-functional) clone frequencies in low biased 5'-  
 240 RACE-based repertoire versus two-side multiplex (VJMplex)-based repertoire obtained for the  
 241 same RNA sample (SRA database, accession numbers SRR3129976 and SRR3129972): before  
 242 and after iROAR processing. d. In-frame (functional) clone frequencies in low biased 5'-RACE-



243 based repertoire versus two-side multiplex (VJMplex)-based repertoire obtained for the same  
244 RNA sample: before and after iROAR processing. SRA database, accession numbers  
245 SRR3129976 and SRR3129970.  $R^2$  is the squared Pearson correlation coefficient. iROAR was  
246 applied only for biased repertoires: artificially biased RACE and VJMplex. e. OARV and OARJ  
247 of test 5'-RACE-based TRB repertoire (Fig.5b) before artificial bias introduction (green dots  
248 and line), biased one (red dots and line) and corrected one by iROAR (blue dots and line).  
249

### 250 OAR-based approach validation

251 The validation of OAR-based amplification bias correction was performed on the TRB  
252 dataset with *in silico* introduced bias generated from real (experimental) low-biased (5'-RACE)  
253 repertoire (Fig 5b). After correction, the OAR-index indicating general repertoire bias expectedly  
254 decreased from 1.81 to 0.76. Interestingly, the OAR independent measure - R-squared value of *in*  
255 *silico* biased and original repertoire correlation raised from 0.5350 to 0.8915 confirming the  
256 substantial reduction of *in silico* introduced quantitative bias. Afterward, we tested our approach  
257 on real paired experimental datasets obtained from the same RNA sample by two different  
258 method types: 5'-RACE and multiplex PCR (Barennes et al., 2020; Liu et al., 2016) (Fig 5c-d,  
259 Fig 6).



260  
261 **Figure 6.** Effect of iROAR-based PCR bias correction in MPlex repertoire on similarity with  
262 low-biased RACE-based repertoire obtained from the same RNA sample. a) Pearson correlation  
263 coefficient; b) R-square measure; c) Morisita-Horn similarity index. \*\*\*\*  $P < 0.0001$  (two-tailed  
264 Wilcoxon matched-pairs signed rank test,  $CI=0.95$ ). Dataset: PRJNA548335 (3 different RACE  
265 (RACE-2, RACE-3, RACE-4 in 6 replicates each) protocols vs. RNA-based MPlex (Multiplex-3)  
266 protocol for Donor1 and Donor2 (100 ng RNA input): total 36 points; PRJNA309577 (One  
267 RACE protocol vs. one MPlex protocol for Donors S01 (4 MPlex replicates vs. 2 RACE  
268 replicates), S02 (2 MPlex replicates vs. 4 RACE replicates) and donor S03 (1 MPlex replicate vs.  
269 1 RACE replicate): total 17 points).

270  
271 As a result of amplification bias correction, OAR index for multiplex-based repertoire  
272 decreased 1.5-fold average. At the exact time, the correlation of clonal frequencies obtained with  
273 RACE and multiplex significantly increased (Pearson correlation measure and R-squared value  
274 increased 1.5-fold average each) with a significant rise of repertoires similarity (Morisita-Horn  
275 index increased 1.7-fold average) (Fig 6). Importantly, amplification bias decreased in both out-

276 of-frame and in-frame clone sets, although normalization coefficients were calculated using out-  
277 of-frame ones only.

278

### 279 **Comparison of iROAR and spike-in-based approach for amplification bias detection**

280 Biological spike-in is considered a classical technique for multiplex PCR bias evaluation.  
281 Several options for this technique including synthetic repertoire (Carlson et al., 2013; Wu et al.,  
282 2020), lymphoid cell lines DNA mix and DNA from human blood, tonsil, and thymus  
283 (Kallemeijn et al., 2018; Knecht et al., 2019) were established to measure V- and J-segment  
284 specific primers performance during TCR/BCR rearrangements amplification in multiplex PCR.  
285 In this study, we compared iROAR-based amplification bias evaluation with a spike-in-based  
286 approach. Similarly to ref. (Kallemeijn et al., 2018; Knecht et al., 2019) we were using natural  
287 thymic cell-derived spike-ins rather than synthetic ones. Human CD8 T-cells derived DNA was  
288 used as a target input for the libraries' preparation. TRA rearrangements library of thymocytes  
289 were used as a source of spike-ins. Two different random mixes of TRAV and TRAJ-specific  
290 primers (0.18-4.7  $\mu$ M each) were used for multiplex PCR amplification of target DNA with  
291 spike-in added. Each test library was prepared in two replicas (four test libraries total). The  
292 obtained libraries were sequenced with an average coverage of 9.88 reads per clonotype and  
293 contained 35 818 – 40 209 target and 2 298 - 3 571 spike-in clonotypes after pseudogenes  
294 removal (Table 1).

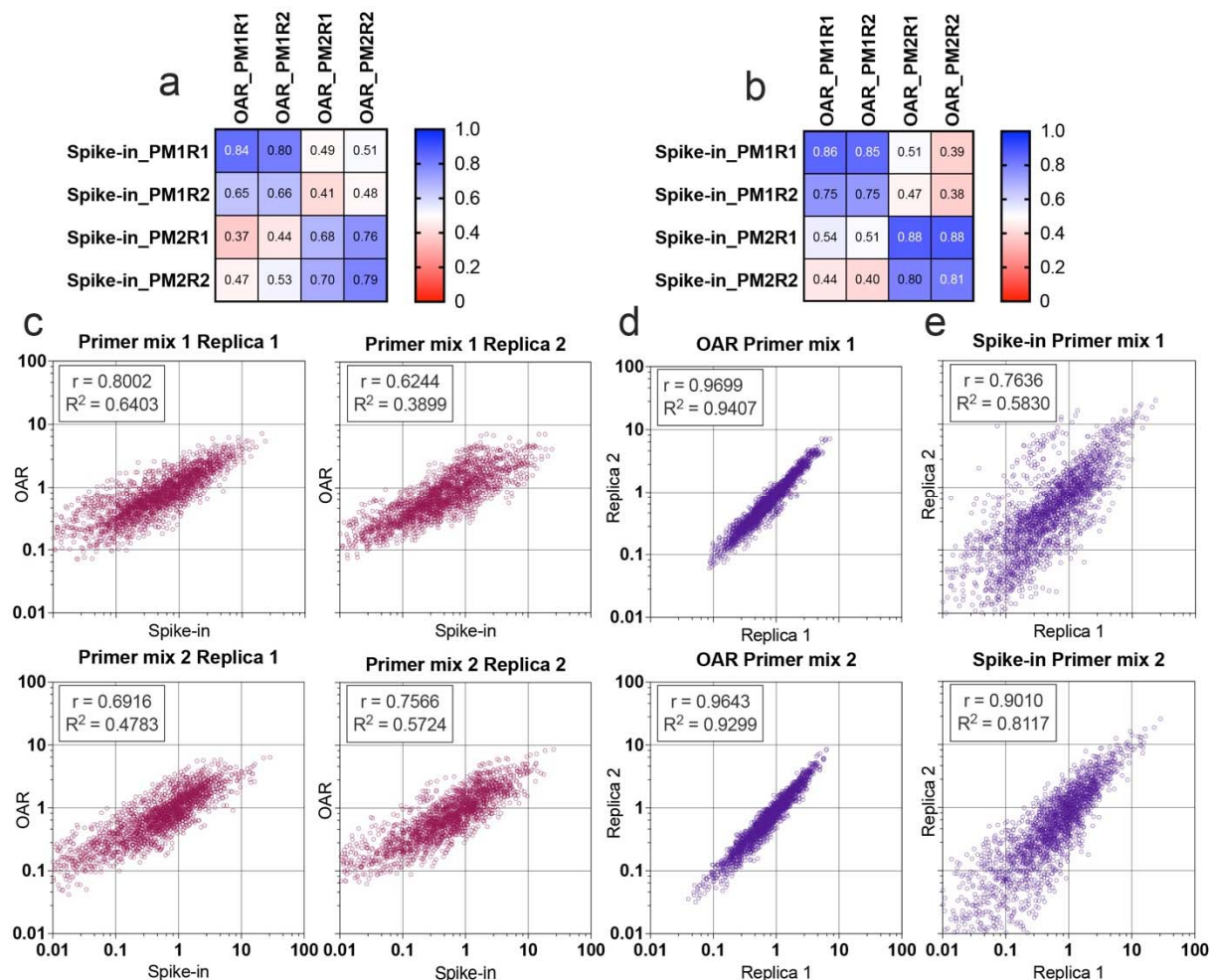
295

296 **Table 1.** The number of spike-in and target clonotypes in test TRA libraries.

Sample	Spike-in clonotypes			Target clonotypes		
	number	read count	coverage	number	read count	coverage
Primer mix 1 Replica 1	3 571	30 474	8.53	39 911	348 792	8.74
Primer mix 1 Replica 2	2 698	19 420	7.20	35 818	303 494	8.47
Primer mix 2 Replica 1	3 439	34 717	10.10	40 209	425 508	10.58
Primer mix 2 Replica 2	2 298	24 823	10.80	33 406	383 615	11.48

297

298 Multiplex PCR bias of each separate V and J-gene was calculated using both iROAR and  
299 biological spike-in approaches demonstrating the high correlation level (Fig 7a and 7b) for the  
300 matched OAR/Spike-in pairs (Pearson's  $r = 0.78$  average) in contrast to mismatched ones  
301 (Pearson's  $r = 0.46$  average). VJ combination bias for both approaches was calculated by  
302 multiplying V and J-segment biases and compared using correlation analysis (Fig 7c-e). iROAR  
303 and spike-in detected VJ biases showed a strong positive correlation (Pearson's  $r = 0.7182$   
304 average) for all four test TRA libraries (Fig 7c). Based on replicas comparison, the  
305 reproducibility of iROAR detected VJ bias was higher than one detected using spike-in control  
306 (Fig 7d and 7e).

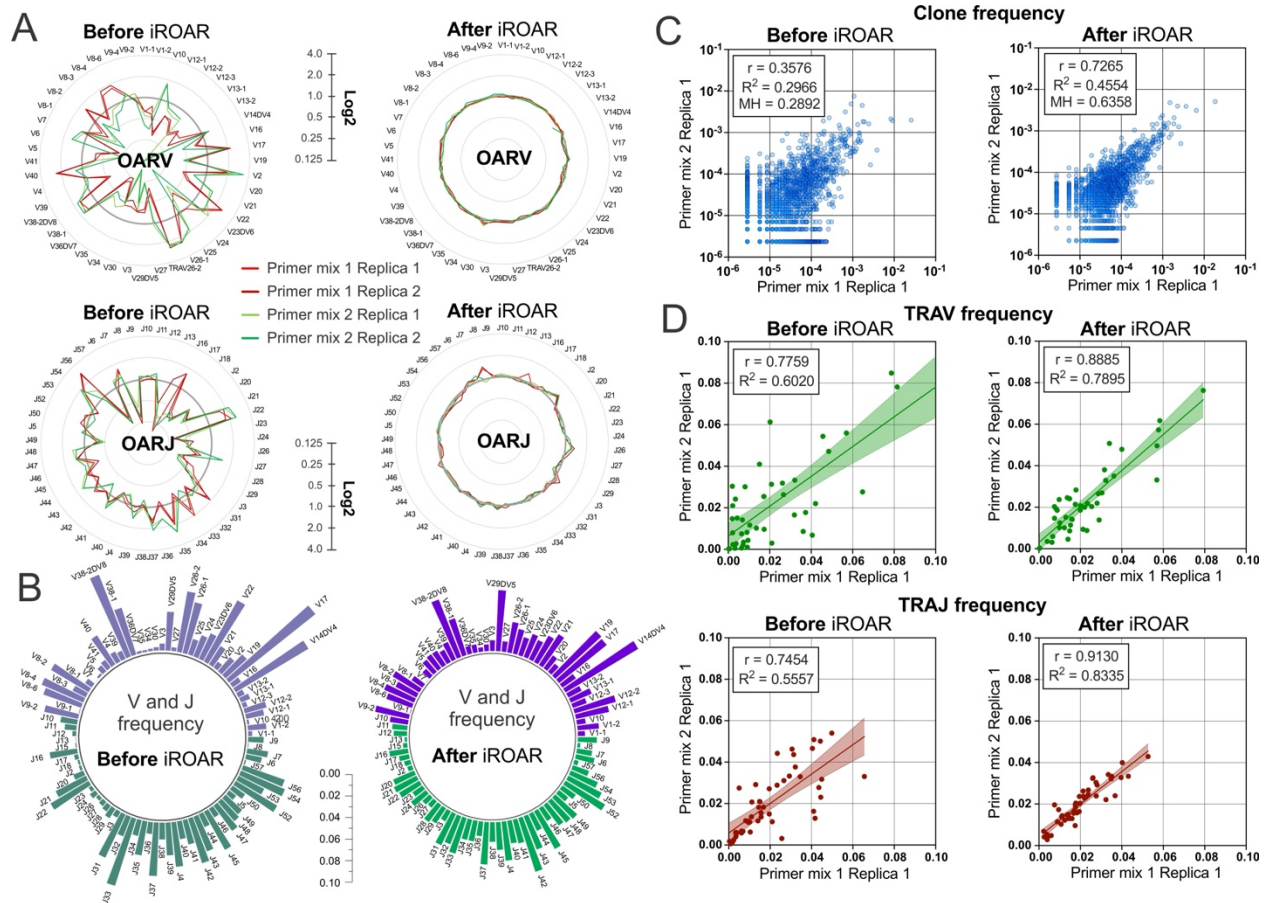


307  
 308 **Figure 7.** Comparison of OAR-based and biological spike-in-based approaches for multiplex  
 309 PCR bias detection. Pearson's correlation coefficient for V-segments bias measure (a) and J-  
 310 segments bias measure (b). Column and row titles: PM = Primer mix, R = replica. c.  
 311 Correlation of VJ combination bias calculated by iROAR and biological spike-ins. d.  
 312 Reproducibility of iROAR-based VJ combination bias detection. e. Reproducibility of Spike-in-  
 313 based VJ combination bias detection. Data: PRJNA825832.

314  
 315 **Impact of iROAR on a similarity of repertoires prepared by different multiplex PCR**  
 316 **systems**

317 To further test the iROAR approach's ability to raise the uniformity of repertoires by  
 318 reducing multiplex PCR-specific bias, we analyzed changes in the similarity of repertoires  
 319 prepared for the same individual but using different multiplex methods. For this purpose, we  
 320 compared OARs, V/J, and clonotype frequencies before and after bias correction using iROAR  
 321 in test TRA libraries prepared with Primer mix 1 and Primer mix 2 (after spike-in removal). As a  
 322 result of iROAR-based bias correction, the difference between OARs for these two library types  
 323 significantly decreases, and OARs themselves approach a value of one. By default, iROAR does  
 324 not affect the diversity of repertoires and does not remove any clonotypes. Meanwhile, V and J

325 frequencies are subject to substantial changes (Fig.8b) depending on the initial bias level. These  
 326 changes occur in both biased repertoires (Primer mix 1 and Primer mix 2) and lead to an increase  
 327 its convergence (Fig.8d). Herewith R squared measure increased 1.31-fold and 1.5-fold for V  
 328 and J-gene frequencies, respectively. Moreover, bias correction using iROAR also increases  
 329 similarities of clone frequencies (Fig.8c). In this case both the Morisita-Horn index and Pearson  
 330 correlation coefficient increase 2-fold, and R squared measure increases 1.5-fold.



331  
 332 **Figure 8.** Convergence of OAR, clonotype, and V/J frequencies between two TRA repertoire  
 333 before and after iROAR based bias correction. a. OAR values changes in four test TRA libraries  
 334 after PCR bias correction using iROAR. b. TRAV and TRAJ frequency changes after PCR bias  
 335 correction using iROAR (Sample: Primer mix 1 Replica 1). c. Correlation of clonal frequencies  
 336 of two different types of test TRA repertoires before and after iROAR-based PCR bias correction.  
 337 d. Correlation of V and J-gene frequencies of test TRA repertoires before and after iROAR-based  
 338 PCR bias correction.

339  
 340 It is important to note that OARs calculation and bias correction for each of the analyzed  
 341 test TRA repertoires was performed entirely independently without the involvement of any  
 342 common normalization coefficients or spike-in controls. Therefore, each repertoire contains  
 343 enough information to correct it adequately, increasing the consistencies of interrogated  
 344 repertoires obtained even by different multiplex PCR protocols.

345 All observed results can be considered evidence of the actual capacity of iROAR  
346 approach to accurately detect and reduce multiplex-specific quantitative bias in adaptive immune  
347 receptor repertoires.

348  
349

## 350 **Discussion**

351 Even a small difference in amplification efficiencies can lead to a massive bias after  
352 multiple amplification cycles due to the exponential nature of PCR. Thus, most of the existing  
353 immune repertoire library preparation methods are subjected to amplification bias. The effect of  
354 distinct PCR bias-generating factors can be reduced experimentally by varying reaction mixture  
355 content and introducing special protocols (UMI, crafty primer structures, spike-in controls).  
356 However, the criteria for estimating and removing the residual bias after applying these  
357 optimization approaches are lacking. Here we close this gap by introducing the OAR value and  
358 OAR-index, which score PCR bias for both V- and J-genes separately (OAR values) and the  
359 whole repertoire dataset (OAR-index). Based on OAR values, we developed the first fully  
360 computational approach to decipher and correct amplification bias in adaptive immune receptor  
361 repertoires produced by one-side or two-side multiplex PCR-based methods, using RNA or DNA  
362 as a template. Due to the inability to use UMI-based correction for DNA-based multiplex, the  
363 developed approach is the only currently available technique allowing direct measuring and  
364 correcting PCR bias in such repertoires without additional experiments.

365 In contrast to cell-line mix spike-in (Knecht et al., 2019) or synthetic repertoire-based  
366 (Carlson et al., 2013; Wu et al., 2020) PCR bias correction, the proposed approach operates with  
367 hundreds and even thousands of natural calibrators (out-of-frame clones) for each V-J gene pair.  
368 It makes this method potentially more reliable due to the ability to minimize the impact of CDR3  
369 structure on PCR bias calculation since out-of-frame captures significantly higher CDR3  
370 diversity than biological spike-ins. Moreover, similarly to a previously described method  
371 (Carlson et al., 2013) the OAR-based approach can also be used for primer efficacy evaluation to  
372 optimize their structures and concentrations, which in turn will straighten the coverage of various  
373 V- and J-genes and minimize the number of experimentally lost clones. Being fully  
374 computational, the developed PCR bias correction algorithm can be easily implemented in any  
375 TCR/BCR repertoire analysis pipeline, noticeably improving the quantitative parts of the  
376 analysis. Even though it's not possible to fully substitute the low-biased RACE methods, iROAR  
377 is capable to make multiplex-PCR-based repertoires more consistent with RACE-based ones.  
378 Therefore, the developed approach can provide the opportunity to compare the immune  
379 repertoire datasets generated using different library preparation methods.

380

## 381 **Methods**

### 382 **Raw-data processing and immune repertoires reconstruction**

383 All sequencing data used in this study represent human TCR and BCR repertoires. The  
384 repertoires (see Suppl. Table 1) were reconstructed from fastq data using MiXCR v2 software

385 (Bolotin et al., 2017, 2015) after primers and adapters trimming using FASTP software (Chen et  
386 al., 2018). All obtained repertoires were converted to VDJTOOLS (Shugay et al., 2015) format  
387 for unification. Erroneous clones generated by single nucleotide substitution were removed from  
388 the repertoire using the “Correct” function from the VDJTOOLS software package. Erroneous  
389 clones generated by single nucleotide indels were removed from repertoires using the “Filter”  
390 function from developed iROAR software. V and J pseudogenes were removed from repertoires  
391 using the “FilterBySegment” function of VDJTOOLS.

392

### 393 **TRA repertoires preparation**

394 The peripheral blood was collected from a healthy volunteer from the article's co-authors  
395 with informed consent in a certified clinical lab. PBMC was separated from whole blood using  
396 the Ficoll-Paque approach. CD8<sup>+</sup> T-cells were isolated using Dynabeads™ CD8 Positive  
397 Isolation Kit (Invitrogen). DNA for library preparation was extracted from CD8<sup>+</sup> T-cells using  
398 FlexiGene DNA Kit (Qiagen). 150 ng aliquots of obtained DNA were used as input to prepare  
399 each out of four TRA libraries. Each DNA aliquot was premixed with 0.1 pg of serial diluted  
400 low-biased TRA library (prepared using MiLaboratories Human TCR kit) of thymic cells (spike-  
401 in matrix) as biological spike-ins. Two pools of previously designed (Komkov et al., 2020)  
402 TRAV and TRAJ-specific primers (MiLaboratories LLC) with randomly selected concentrations  
403 (0.18-4.7  $\mu$ M each) were generated to produce two types of TRA libraries with different  
404 quantitative bias status simulating libraries produced by different multiplex PCR methods.  
405 Library preparation was performed according to the protocol from ref. (Komkov et al., 2020).  
406 Both types of TRA libraries were prepared in two replicas and sequenced along with a spike-in  
407 matrix library on the MiSeq Illumina instrument (SE 150 nt) with moderate coverage 480 000  
408 reads per library.

409

### 410 **Biological spike-in detection and analysis**

411 TRA repertoires were extracted from FASTQ files using MIXCR software. All obtained  
412 MIXCR output files were converted to VDJTOOLS format as described above. Extraction of the  
413 spike-in sequences and spike-in free repertoires from sequenced libraries was performed using  
414 the VDJTOOLS function “ApplySampleAsFilter” and the sequenced spike-in library as a filter.  
415 Spike-in-based amplification bias was calculated as the quotient of V and J-frequency in spike-  
416 ins extracted from target libraries and corresponding V and J-frequency in the spike-in matrix,  
417 which was not subjected to multiplex amplification. OARs for obtained TRA libraries were  
418 calculated using iROAR software and spike-in-free repertoires as input. VJ bias values were  
419 calculated by multiplying V- to J-segment-specific biases. Correlation analysis of iROAR and  
420 Spike-in VJ bias values was performed using GraphPad Prism9 software.

421

### 422 **Step-by-step pipeline for the OAR evaluation used in this study**

- 423 1) Single nucleotide error correction in read1/read2 intersected sequences and Illumina  
424 adapters removal (optional):

```
425 fastp -c -i input_R1.fastq.gz -I input_R2.fastq.gz -o fp.input_R1.fastq.gz -O fp.input_R2.fastq.gz
426     2) Raw reads alignment (essential):
427         a) For TCR beta chains
428 mixcr align -c TRB fp.input_R1.fastq.gz fp.input_R2.fastq.gz output1.vdjca
429         b) For TCR beta chains
430 mixcr align -c TRA fp.input_R1.fastq.gz fp.input_R2.fastq.gz output1.vdjca
431     3) Clonotypes assemble (essential):
432 mixcr assemble output1.vdjca output2.clns
433     4) TCR repertoire export in a human-readable format (essential):
434 mixcr exportClones output2.clns clones.txt
435     5) Convert repertoire into VDJtools format (essential):
436 java -jar vjdjtools.jar Convert -S mixcr clones.txt vjdjtools
437     6) Artificial diversity removal by single nucleotide substitutions correction (optional):
438 java -jar vjdjtools.jar Correct vjdjtools.clones.txt correct
439     7) Pseudogenes removal (optional):
440         a) For TCR beta chains
441 java -jar vjdjtools.jar FilterBySegment --j-segment TRBJ2-2P --v-segment TRBV1,TRBV12-
442 1,TRBV12-2,TRBV17,TRBV21-1,TRBV22-1,TRBV23-1,TRBV26,TRBV5-2,TRBV5-
443 3,TRBV5-7,TRBV6-7,TRBV7-1,TRBV7-5,TRBV8-1,TRBV8-2 --negative
444 correct.vjdjtools.clones.txt filter
445         b) For TCR alpha chains
446 java -jar vjdjtools.jar FilterBySegment --j-segment
447 TRAJ1,TRAJ19,TRAJ2,TRAJ25,TRAJ51,TRAJ55,TRAJ58,TRAJ59,TRAJ60,TRAJ61 --v-
448 segment TRAV11,TRAV11-1,TRAV14-
449 1,TRAV15,TRAV28,TRAV31,TRAV32,TRAV33,TRAV37,TRAV46,TRAV8-5,TRAV8-6-
450 1,TRAV8-7 --negative correct.vjdjtools.clones.txt filter
451     8) Artificial diversity removal by single nucleotide indels correction (optional):
452 iroar Filter -se 0.01 filter.correct.vjdjtools.clones.txt filter2.txt
453     9) OARs calculation and quantitative bias correction (essential):
454 iroar Count -min_outframe 15 -r -z 1 -iter 1 -mt 1 input_folder output_folder
455 (input_folder must contain filter2.txt file)
456
457
```

### **OAR evaluation and statistical analysis**

459 For the OAR and OAR-index calculation and amplification bias removal, we used the  
460 command-line-based iROAR software designed in this study and freely available for nonprofit  
461 use at GitHub (<https://github.com/smiranast/iROAR>). For the OAR comparison between 5'-  
462 RACE, one-side, and two-side multiplex PCRs, an equal number of out-of-frame clones (50,000)  
463 was randomly selected from TCR repertoires of 15 healthy individuals (for each approach).  
464 Average population V- and J-gene frequencies (unweighted) were calculated based on out-of-

465 frame clones from 105 TRB repertoires obtained by two methods: 5'-RACE (95 repertoires) and  
466 single-cell TCR profiling (10X genomics) (10 repertoires) (Suppl. Table 1) using the  
467 “CalcSegmentUsage” function with “-u” parameter of VDJTOOLS. All statistical tests were  
468 performed using Prism9 GraphPad software (<https://www.graphpad.com/>).

469

#### 470 **iROAR software requirement**

471 Recommended system configuration for iROAR running: Linux or MacOS, 2 CPU, 8GB RAM,  
472 programming language: python=3.7.3, required Python packages: matplotlib=3.0.3,  
473 numpy=1.16.2, pandas=0.24.2, requests=2.21.0. Starting iROAR package includes list of  
474 average populational frequencies with standard deviations of TRB and TRA V- and J-genes  
475 related to the European population. iROAR run command: iroar Count [optional parameters]  
476 <input> <output>. Recommended parameters for most tasks: -min\_outframe 15 -r -z 1 -iter 1 -mt  
477 1. Full list of available parameters is deposited in project directory at github  
478 (<https://github.com/smiranast/iROAR>)

479

480

#### 481 **Data access**

482 All analyzed datasets were downloaded from open-source databases: NCBI SRA  
483 (<https://www.ncbi.nlm.nih.gov/sra>), ENA (<https://www.ebi.ac.uk/ena>), and Zenodo project  
484 (<https://zenodo.org/>). A complete list of web links and accession numbers is summarized in  
485 Suppl. Table 1. TRA repertoire dataset generated in this study for iROAR validation is available  
486 under access number PRJNA825832.

487 The iROAR software and its documentation are available at the link:  
488 <https://github.com/smiranast/iROAR>. The additional software used in this study is available in  
489 the GitHub repository (<https://github.com/milaboratory/mixcr>,  
490 <https://github.com/mikessh/vdjtools>, <https://github.com/OpenGene/fastp>)

491

#### 492 **Funding**

493 This work was supported by Russian Science Foundation [grant 20-75-10091 to A.K.],  
494 the analysis of TRA Mplex data was supported by Russian Foundation for Basic Research [grant  
495 20-015-00462 to A.K.].

496

#### 497 **Acknowledgments**

498 We thank Grigory Armeev and Valery Novoseletsky for their help with data storage and  
499 processing.

500

#### 501 **Competing interest statement**

502 MiLaboratories LLC (USA) holds the rights on the TRA-specific oligonucleotide  
503 sequences used in this study. The authors declare that they have no other competing interests.

504



505 **Supplementary Data**

506 **Supplementary Table 1.** XLSX. The file contains accession numbers and links to the datasets  
507 used in this study.

508 **Supplementary Table 2.** XLSX. Comparison of iROAR algorithm with the existing approaches  
509 for PCR bias removal in human adaptive immune receptor repertoires

510 **Supplementary Figure 1.** JPEG. V- and J-gene frequencies among unique out-of-frame  
511 rearrangements calculated using biased (two-side multiplex, empty circles) and low-biased  
512 (RACE, filled circles) are compared to average population frequencies (violin plot). Significantly  
513 biased V and J genes are highlighted pink. Paired (the same starting RNA samples) two-side  
514 multiplex and RACE data: SRA accession number PRJNA309577, average population  
515 frequencies were calculated using a series of RACE TCR and single-cell TCRseq data (see  
516 Suppl. Table 1).

517

518

519 **References**

520 Barennes P, Quiniou V, Shugay M, Egorov ES, Davydov AN, Chudakov DM, Uddin I, Ismail  
521 M, Oakes T, Chain B, Eugster A, Kashofer K, Rainer PP, Darko S, Ransier A, Douek  
522 DC, Klatzmann D, Mariotti-Ferrandiz E. 2020. Benchmarking of T cell receptor  
523 repertoire profiling methods reveals large systematic biases. *Nat Biotechnol.*  
524 doi:10.1038/s41587-020-0656-3

525 Bolotin DA, Poslavsky S, Davydov AN, Frenkel FE, Fanchi L, Zolotareva OI, Hemmers S,  
526 Putintseva EV, Obraztsova AS, Shugay M, Ataullakhanov RI, Rudensky AY,  
527 Schumacher TN, Chudakov DM. 2017. Antigen receptor repertoire profiling from RNA-  
528 seq data. *Nat Biotechnol* **35**:908–911. doi:10.1038/nbt.3979

529 Bolotin DA, Poslavsky S, Mitrophanov I, Shugay M, Mamedov IZ, Putintseva EV, Chudakov  
530 DM. 2015. MiXCR: software for comprehensive adaptive immunity profiling. *Nat*  
531 *Methods* **12**:380–381. doi:10.1038/nmeth.3364

532 Brüggemann M, Kotrová M, Knecht H, Bartram J, Boudjoghra M, Bystry V, Fazio G, Froňková  
533 E, Giraud M, Grioni A, Hancock J, Herrmann D, Jiménez C, Krejci A, Moppett J, Reigl  
534 T, Salson M, Scheijen B, Schwarz M, Songia S, Svaton M, van Dongen JJM, Villarese P,  
535 Wakeman S, Wright G, Cazzaniga G, Davi F, García-Sanz R, Gonzalez D, Groenen  
536 PJTA, Hummel M, Macintyre EA, Stamatopoulos K, Pott C, Trka J, Darzentas N,  
537 Langerak AW, EuroClonality-NGS working group. 2019. Standardized next-generation  
538 sequencing of immunoglobulin and T-cell receptor gene recombinations for MRD marker  
539 identification in acute lymphoblastic leukaemia; a EuroClonality-NGS validation study.  
540 *Leukemia* **33**:2241–2253. doi:10.1038/s41375-019-0496-7

541 Carlson CS, Emerson RO, Sherwood AM, Desmarais C, Chung M-W, Parsons JM, Steen MS,  
542 LaMadrid-Herrmannsfeldt MA, Williamson DW, Livingston RJ, Wu D, Wood BL,  
543 Rieder MJ, Robins H. 2013. Using synthetic templates to design an unbiased multiplex  
544 PCR assay. *Nat Commun* **4**:2680. doi:10.1038/ncomms3680

- 545 Chen S, Zhou Y, Chen Y, Gu J. 2018. fastp: an ultra-fast all-in-one FASTQ preprocessor.  
546 *Bioinforma Oxf Engl* **34**:i884–i890. doi:10.1093/bioinformatics/bty560
- 547 Gee MH, Han A, Lofgren SM, Beausang JF, Mendoza JL, Birnbaum ME, Bethune MT, Fischer  
548 S, Yang X, Gomez-Eerland R, Bingham DB, Sibener LV, Fernandes RA, Velasco A,  
549 Baltimore D, Schumacher TN, Khatri P, Quake SR, Davis MM, Garcia KC. 2018.  
550 Antigen Identification for Orphan T Cell Receptors Expressed on Tumor-Infiltrating  
551 Lymphocytes. *Cell* **172**:549-563.e16. doi:10.1016/j.cell.2017.11.043
- 552 Goncharov MM, Bryushkova EA, Sharaev NI, Skatova VD, Baryshnikova AM, Sharonov GV,  
553 Karnaukhov V, Vakhitova MT, Samoylenko IV, Demidov LV, Lukyanov S, Chudakov  
554 DM, Serebrovskaya EO. 2022. Pinpointing the tumor-specific T cells via TCR clusters.  
555 *eLife* **11**:e77274. doi:10.7554/eLife.77274
- 556 Huang J, Alexey S, Li J, Jones T, Grande G, Douthit L, Xie Jun, Chen D, Wu X, Michael M,  
557 Xiao C, Zhao J, Xie X, Xie Jia, Chen XL, Fu G, Alexander G, Tzeng C-M. 2019. Unique  
558 CDR3 epitope targeting by CAR-T cells is a viable approach for treating T-cell  
559 malignancies. *Leukemia* **33**:2315–2319. doi:10.1038/s41375-019-0455-3
- 560 Kallemijn MJ, Kavelaars FG, van der Klift MY, Wolvers-Tettero ILM, Valk PJM, van Dongen  
561 JJM, Langerak AW. 2018. Next-Generation Sequencing Analysis of the Human TCR $\gamma\delta$ +  
562 T-Cell Repertoire Reveals Shifts in V $\gamma$ - and V $\delta$ -Usage in Memory Populations upon  
563 Aging. *Front Immunol* **9**:448. doi:10.3389/fimmu.2018.00448
- 564 Knecht H, Reigl T, Kotrová M, Appelt F, Stewart P, Bystry V, Krejci A, Grioni A, Pal K,  
565 Stranska K, Plevova K, Rijntjes J, Songia S, Svatoň M, Froňková E, Bartram J, Scheijen  
566 B, Herrmann D, García-Sanz R, Hancock J, Moppett J, van Dongen JJM, Cazzaniga G,  
567 Davi F, Groenen PJTA, Hummel M, Macintyre EA, Stamatopoulos K, Trka J, Langerak  
568 AW, Gonzalez D, Pott C, Brüggemann M, Darzentas N, EuroClonality-NGS Working  
569 Group. 2019. Quality control and quantification in IG/TR next-generation sequencing  
570 marker identification: protocols and bioinformatic functionalities by EuroClonality-NGS.  
571 *Leukemia* **33**:2254–2265. doi:10.1038/s41375-019-0499-4
- 572 Komkov A, Miroshnichenkova A, Nugmanov G, Popov A, Pogorelyy M, Zapletalova E,  
573 Jelinkova H, Pospisilova S, Lebedev Y, Chudakov D, Olshanskaya Y, Plevova K,  
574 Maschan M, Mamedov I. 2020. High-throughput sequencing of T-cell receptor alpha  
575 chain clonal rearrangements at the DNA level in lymphoid malignancies. *Br J Haematol*  
576 **188**:723–731. doi:10.1111/bjh.16230
- 577 Liu X, Zhang W, Zeng X, Zhang R, Du Y, Hong X, Cao H, Su Z, Wang C, Wu J, Nie C, Xu X,  
578 Kristiansen K. 2016. Systematic Comparative Evaluation of Methods for Investigating  
579 the TCR $\beta$  Repertoire. *PLoS One* **11**:e0152464. doi:10.1371/journal.pone.0152464
- 580 Ma K-Y, He C, Wendel BS, Williams CM, Xiao J, Yang H, Jiang N. 2018. Immune Repertoire  
581 Sequencing Using Molecular Identifiers Enables Accurate Clonality Discovery and Clone  
582 Size Quantification. *Front Immunol* **9**:33. doi:10.3389/fimmu.2018.00033
- 583 Mamedov IZ, Britanova OV, Zvyagin IV, Turchaninova MA, Bolotin DA, Putintseva EV,  
584 Lebedev YB, Chudakov DM. 2013. Preparing unbiased T-cell receptor and antibody

- 585 cDNA libraries for the deep next generation sequencing profiling. *Front Immunol* **4**:456.  
586 doi:10.3389/fimmu.2013.00456
- 587 Minervina A, Pogorelyy M, Mamedov I. 2019. T-cell receptor and B-cell receptor repertoire  
588 profiling in adaptive immunity. *Transpl Int Off J Eur Soc Organ Transplant* **32**:1111–  
589 1123. doi:10.1111/tri.13475
- 590 Minervina AA, Komech EA, Titov A, Bensouda Koraichi M, Rosati E, Mamedov IZ, Franke A,  
591 Efimov GA, Chudakov DM, Mora T, Walczak AM, Lebedev YB, Pogorelyy MV. 2021.  
592 Longitudinal high-throughput TCR repertoire profiling reveals the dynamics of T-cell  
593 memory formation after mild COVID-19 infection. *eLife* **10**:e63502.  
594 doi:10.7554/eLife.63502
- 595 Minervina AA, Pogorelyy MV, Komech EA, Karnaukhov VK, Bacher P, Rosati E, Franke A,  
596 Chudakov DM, Mamedov IZ, Lebedev YB, Mora T, Walczak AM. 2020. Primary and  
597 secondary anti-viral response captured by the dynamics and phenotype of individual T  
598 cell clones. *eLife* **9**. doi:10.7554/eLife.53704
- 599 Murugan A, Mora T, Walczak AM, Callan CG. 2012. Statistical inference of the generation  
600 probability of T-cell receptors from sequence repertoires. *Proc Natl Acad Sci U S A*  
601 **109**:16161–16166. doi:10.1073/pnas.1212755109
- 602 Nazarov VI, Minervina AA, Komkov AY, Pogorelyy MV, Maschan MA, Olshanskaya YV,  
603 Zvyagin IV, Chudakov DM, Lebedev YB, Mamedov IZ. 2016. Reliability of immune  
604 receptor rearrangements as genetic markers for minimal residual disease monitoring.  
605 *Bone Marrow Transplant* **51**:1408–1410. doi:10.1038/bmt.2016.148
- 606 Oakes T, Heather JM, Best K, Byng-Maddick R, Husovsky C, Ismail M, Joshi K, Maxwell G,  
607 Noursadeghi M, Riddell N, Ruehl T, Turner CT, Uddin I, Chain B. 2017. Quantitative  
608 Characterization of the T Cell Receptor Repertoire of Naïve and Memory Subsets Using  
609 an Integrated Experimental and Computational Pipeline Which Is Robust, Economical,  
610 and Versatile. *Front Immunol* **8**:1267. doi:10.3389/fimmu.2017.01267
- 611 Oliveira G, Stromhaug K, Klaeger S, Kula T, Frederick DT, Le PM, Forman J, Huang T, Li S,  
612 Zhang W, Xu Q, Cieri N, Clauser KR, Shukla SA, Neuberg D, Justesen S, MacBeath G,  
613 Carr SA, Fritsch EF, Hacohen N, Sade-Feldman M, Livak KJ, Boland GM, Ott PA,  
614 Keskin DB, Wu CJ. 2021. Phenotype, specificity and avidity of antitumour CD8+ T cells  
615 in melanoma. *Nature* **596**:119–125. doi:10.1038/s41586-021-03704-y
- 616 Pogorelyy MV, Minervina AA, Touzel MP, Sycheva AL, Komech EA, Kovalenko EI,  
617 Karganova GG, Egorov ES, Komkov AY, Chudakov DM, Mamedov IZ, Mora T,  
618 Walczak AM, Lebedev YB. 2018. Precise tracking of vaccine-responding T cell clones  
619 reveals convergent and personalized response in identical twins. *Proc Natl Acad Sci U S*  
620 *A* **115**:12704–12709. doi:10.1073/pnas.1809642115
- 621 Robins HS, Campregher PV, Srivastava SK, Wachter A, Turtle CJ, Kahsai O, Riddell SR,  
622 Warren EH, Carlson CS. 2009. Comprehensive assessment of T-cell receptor beta-chain  
623 diversity in alphabeta T cells. *Blood* **114**:4099–4107. doi:10.1182/blood-2009-04-217604

- 624 Shugay M, Bagaev DV, Turchaninova MA, Bolotin DA, Britanova OV, Putintseva EV,  
625 Pogorelyy MV, Nazarov VI, Zvyagin IV, Kirgizova VI, Kirgizov KI, Skorobogatova EV,  
626 Chudakov DM. 2015. VDJtools: Unifying Post-analysis of T Cell Receptor Repertoires.  
627 *PLoS Comput Biol* **11**:e1004503. doi:10.1371/journal.pcbi.1004503
- 628 Sycheva AL, Komech EA, Pogorelyy MV, Minervina AA, Urazbakhtin SZ, Salnikova MA,  
629 Vorovitch MF, Kopantzev EP, Zvyagin IV, Komkov AY, Mamedov IZ, Lebedev YB.  
630 2022. Inactivated tick-borne encephalitis vaccine elicits several overlapping waves of T  
631 cell response. *Front Immunol* **13**.
- 632 Sycheva AL, Pogorelyy MV, Komech EA, Minervina AA, Zvyagin IV, Staroverov DB,  
633 Chudakov DM, Lebedev YB, Mamedov IZ. 2018. Quantitative profiling reveals minor  
634 changes of T cell receptor repertoire in response to subunit inactivated influenza vaccine.  
635 *Vaccine* **36**:1599–1605. doi:10.1016/j.vaccine.2018.02.027
- 636 Tirtakusuma R, Szoltysek K, Milne P, Grinev V, Ptasinaska A, Chin PS, Meyer C, Nakjang S,  
637 Hehir-Kwa JY, Williamson D, Cauchy P, Keane P, Assi SA, Ashtiani M, Kellaway SG,  
638 Imperato MR, Vogiatzi F, Schweighart-James EK, Lin S, Wunderlich M, Stutterheim J,  
639 Komkov A, Zerkalenskova E, Evans P, McNeill HV, Elder A, Martínez-Soria N, Fordham  
640 SE, Shi Y, Russell LJ, Pal D, Smith AG, Kingsbury Z, Becq J, Eckert C, Haas OA, Carey  
641 P, Bailey S, Skinner R, Miakova N, Collin M, Bigley V, Haniffa M, Marschalek R,  
642 Harrison CJ, Cargo CA, Schewe DM, Olshanskaya Y, Thirman MJ, Cockerill PN,  
643 Mulloy JC, Blair HJ, Vormoor HJ, Allan JM, Bonifer C, Heidenreich O, Bomken S.  
644 2022. Epigenetic regulator genes direct lineage switching in MLL/AF4 leukaemia. *Blood*  
645 *blood.2021015036*. doi:10.1182/blood.2021015036
- 646 Wang B, DeKosky BJ, Timm MR, Lee J, Normandin E, Misasi J, Kong R, McDaniel JR,  
647 Delidakis G, Leigh KE, Niezold T, Choi CW, Viox EG, Fahad A, Cagigi A, Ploquin A,  
648 Leung K, Yang ES, Kong W-P, Voss WN, Schmidt AG, Moody MA, Ambrozak DR,  
649 Henry AR, Laboune F, Ledgerwood JE, Graham BS, Connors M, Douek DC, Sullivan  
650 NJ, Ellington AD, Mascola JR, Georgiou G. 2018. Functional interrogation and mining  
651 of natively paired human VH:VL antibody repertoires. *Nat Biotechnol* **36**:152–155.  
652 doi:10.1038/nbt.4052
- 653 Wang C, Sanders CM, Yang Q, Schroeder HW, Wang E, Babrzadeh F, Gharizadeh B, Myers  
654 RM, Hudson JR, Davis RW, Han J. 2010. High throughput sequencing reveals a complex  
655 pattern of dynamic interrelationships among human T cell subsets. *Proc Natl Acad Sci U*  
656 *S A* **107**:1518–1523. doi:10.1073/pnas.0913939107
- 657 Weinberger J, Jimenez-Heredia R, Schaller S, Suessner S, Sunzenauer J, Reindl-Schwaighofer  
658 R, Weiss R, Winkler S, Gabriel C, Danzer M, Oberbauer R. 2015. Immune Repertoire  
659 Profiling Reveals that Clonally Expanded B and T Cells Infiltrating Diseased Human  
660 Kidneys Can Also Be Tracked in Blood. *PloS One* **10**:e0143125.  
661 doi:10.1371/journal.pone.0143125
- 662 Wilson TL, Kim H, Chou C-H, Langfitt D, Mettelman RC, Minervina AA, Allen EK, Metais J-  
663 Y, Pogorelyy MV, Riberdy JM, Velasquez MP, Kottapalli P, Trivedi S, Olsen SR,

- 664           Lockey T, Willis C, Meagher MM, Triplett BM, Talleur AC, Gottschalk S, Crawford JC,  
665           Thomas PG. 2022. Common trajectories of highly effective CD19-specific CAR T cells  
666           identified by endogenous T cell receptor lineages. *Cancer Discov* candisc.1508.2021.  
667           doi:10.1158/2159-8290.CD-21-1508
- 668   Wood B, Wu D, Crossley B, Dai Y, Williamson D, Gawad C, Borowitz MJ, Devidas M,  
669           Maloney KW, Larsen E, Winick N, Raetz E, Carroll WL, Hunger SP, Loh ML, Robins  
670           H, Kirsch I. 2018. Measurable residual disease detection by high-throughput sequencing  
671           improves risk stratification for pediatric B-ALL. *Blood* **131**:1350–1359.  
672           doi:10.1182/blood-2017-09-806521
- 673   Wu J, Wang Xie, Lin L, Li X, Liu S, Zhang W, Luo L, Wan Z, Fang M, Zhao Y, Wang  
674           Xiaodong, Mai H, Yuan X, Wen F, Li C, Liu X. 2020. Developing an Unbiased  
675           Multiplex PCR System to Enrich the TRB Repertoire Toward Accurate Detection in  
676           Leukemia. *Front Immunol* **11**:1631. doi:10.3389/fimmu.2020.01631  
677